Pseudospin order in monolayer, bilayer and double-layer graphene

IOP Publishing Physica Scripta
Phys. Scr. **T146** (2012) 014012 (9pp) doi:10.1088/0031-8949/2012/T146/014012

Pseudospin order in monolayer, bilayer and double-layer graphene

A H MacDonald, Jeil Jung and Fan Zhang

Department of Physics, University of Texas at Austin, Austin, TX 78712, USA

E-mail: macd@physics.utexas.edu

Received 16 August 2011
Accepted for publication 19 September 2011
Published 31 January 2012
Online at stacks.iop.org/PhysScr/T146/014012

Abstract
Graphene is a gapless semiconductor in which conduction and valence band wavefunctions differ only in the phase difference between their projections onto the two sublattices of the material's two-dimensional honeycomb crystal structure. We explain why this circumstance creates openings for broken symmetry states, including antiferromagnetic states in monolayer and bilayer graphene and exciton condensates in double-layer graphene, which are momentum space analogues of the real-space order common in systems with strong local interactions. We discuss some similarities among, and some differences between, these three broken symmetry states.

PACS numbers: 73.43.−f, 71.10.−w, 73.21.−b, 75.76.−j

(Some figures may appear in colour only in the online journal)

1. Introduction

Graphene [1, 2] is a two-dimensional (2D) crystal consisting entirely of carbon atoms. Its honeycomb lattice is stabilized primarily by strong planar sp^2 bonds, leaving one weakly bonded π-orbital per carbon atom available for metallic conduction. Because of the two atoms per unit cell in a honeycomb lattice the π electrons form two bands, one of which is occupied in a neutral sheet. Because the π-bands cross at the inequivalent honeycomb lattice Brillouin-zone (BZ) corners, i.e. at the K and K' BZ corner points, the gap between the occupied π valence band and the unoccupied π conduction band vanishes. Most of the graphene properties of interest to condensed-matter physicists, for example transport and optical properties, directly involve only the π electron orbitals that are close to the band crossing points. These are accurately described over an energy interval several eV in width by a $\vec{k}\cdot\vec{p}$ Hamiltonian that has the form of a massless Dirac equation:

$$\mathcal{H}_{\rm band} = \hbar v_0 \sum_{\vec{k},s',s} c^{\dagger}_{\vec{k},s'}(\vec{k}\cdot\vec{\sigma}_{s's})c_{\vec{k},s}. \qquad (1)$$

In equation (1) v_0 is the velocity of band electrons at the band-crossing (Dirac) point which can be related to band Hamiltonian π-electron hopping amplitudes, and $\vec{\sigma}$ are Pauli matrices that act on sublattice labels $s(s')$. Equation (1) applies near the valley K Dirac point; the corresponding equation for valley K' is obtained by letting $k_x \to -k_x$. When the sublattice degree-of-freedom is viewed as a pseudospin, we see from equation (1) that the band eigenstates are chiral. In the conduction band of valley K, pseudospin is parallel to the momentum, while in the valence band, pseudospin is antiparallel to the momentum.

Because only one of the two band states is occupied at each momentum, the many-body ground state can be continuously deformed relative to the non-interacting ground state without breaking translational symmetry simply by rotating the pseudospin direction at each momentum. When interactions are neglected the valence band is full, implying that the pseudospin direction is always opposite to the direction of momentum. Since the interaction energy is minimized when all pseudospins are parallel, as we will discuss explicitly below, there is tension between band energy minimization and interaction energy minimization in monolayer graphene. A similar tension arises in two other graphene-based two-dimensional electron systems (2DES)—graphene bilayers [3] which consist of two Bernal stacked graphene layers and graphene double-layers [4] which consist of two layers separated by an insulating tunnel barrier. In this paper, we will discuss the competition between interaction and band energies in all three systems using a

common mean-field language which enables us to highlight similarities and point out differences. We will discuss the potential broken symmetry states using a mean-field theory in which the ground state is determined by minimizing the total energy of single Slater-determinant many-body states varying the pseudospin direction at each momentum $\vec{k}$. By performing a stability analysis for the resulting energy functional we conclude that broken symmetry states can occur in monolayer graphene if interactions are sufficiently strong and that they occur in bilayer and double-layer graphene for interactions of any strength. Our mean-field theory treats the gapped [5–7] and nematic states [8, 9] that have been discussed for bilayer graphene on an equal footing.

A parallel can be drawn between the π-orbital states in these three graphene systems and the electronic states of Mott insulators. In Mott insulators strong interactions project most of the many-electron wavefunction onto a subspace with one atom per unit cell. The only degree-of-freedom that is available in this subspace is the spin state at each lattice position. Unless interactions between spin orientations on different lattice sites are frustrated, the ground state is normally close to the classical ground state in which spin orientations are fixed on each site and chosen to minimize the expectation value of the effective spin Hamiltonian. Quantum fluctuations of spin orientations play only a quantitative role. For the graphene states discussed here the pseudospin energy function that is fixed by energy minimization plays a role similar to the spin distribution in an insulator, but is a function of momentum rather than position. The graphene system band Hamiltonians, which differ essentially in the three cases, act like momentum-dependent pseudospin fields. Because the band Hamiltonians reduce symmetries, energy minimization does not in all cases imply broken symmetry ground states.

Because of the absence of a gap in the graphene case, important quantum fluctuations occur both in pseudospin orientations and in the occupation numbers of momentum states, but we expect that their role is also only quantitative and we do not discuss them at length in this paper. The broken symmetry states that can occur in these graphene systems are unusual from several points of view. For a given spin and valley, the ordered states of both monolayer and bilayer graphene have large quasiparticle Berry curvature and spontaneous quantized anomalous Hall effects [10–14]. The potential broken symmetry states of double-layer graphene have spontaneous interlayer phase coherence, which leads to the suite of phenomena connected with counter-flow superfluidity [15, 16] when the layers are separately contacted.

This paper is organized as follows. In section 2, we formulate the mean-field theory in the three graphene-based 2DES in terms of energy minimization with respect to $\vec{k}$-dependent pseudospin orientation. In sections 3–5, we discuss a stability analysis of the energy functional at the band state configuration for monolayer, bilayer and double-layer systems, respectively, and comment on the character of the broken-symmetry states that result. Finally, in section 6, we point out important similarities and differences between the three cases.

2. Pseudospins in monolayer, bilayer and double-layer graphene

We consider a variational single-Slater-determinant wavefunction with a single pseudospin state occupied at each momentum $\vec{k}$, and minimize the expectation value of the Hamiltonian with respect to the pseudospin orientations $\hat{n}_{\vec{k}}$. In this approximation, the four spin-valley flavors interact only through their contribution to the electrostatic Hartree energy. Since we will consider only states that are locally electrically neutral, we will ignore the Hartree energy for the moment and return to it later when we discuss the role of spin-valley flavors.

It will be convenient to express the band Hamiltonian as an effective magnetic field that acts on the pseudospin degree-of-freedom by writing

$$\mathcal{H}_{\rm band} = \sum_{\vec{k},s',s} c^{\dagger}_{\vec{k},s'} (\vec{h}_{\vec{k}} \cdot \vec{\sigma}_{s's}) c_{\vec{k},s}. \tag{2}$$

In this language, the three cases we discuss are distinguished by their pseudospin effective magnetic fields:

$$\begin{aligned} \vec{h}^{\rm (ML)}_{\vec{k}} &= \hbar v_0 k\, [\cos(\phi_{\vec{k}})\, \hat{x} + \sin(\phi_{\vec{k}})\, \hat{y}], \\ \vec{h}^{\rm (BL)}_{\vec{k}} &= -(\hbar^2 k^2/2m^*)\, [\cos(2\phi_{\vec{k}})\, \hat{x} + \sin(2\phi_{\vec{k}})\, \hat{y}], \\ \vec{h}^{\rm (DL)}_{\vec{k}} &= \hbar v_0 (k - k_F)\, \hat{z}, \end{aligned} \tag{3}$$

for monolayer, bilayer and double-layer cases, respectively. Here $\phi_{\vec{k}}$ is the angular orientation of the 2D $\vec{k}$ momentum and k is its magnitude. Note that the band Hamiltonians are off-diagonal in the pseudospin index in the monolayer and bilayer cases, and diagonal in the double-layer case. The pseudospin labels in equation (2) refer to the sublattice index in the monolayer graphene case and to the layer index in the bilayer and double-layer cases. The form we have chosen for the bilayer Hamiltonian applies only at energies smaller than the interlayer hopping energy γ_1 and is due [3] to virtual hopping between the two low-energy bilayer π-orbital sites, which are located in different layers, via two higher-energy π-orbital sites that are not explicitly retained. Because the pseudospin labels refer to position in all three cases, the electron–electron interaction Hamiltonian is diagonal in pseudospin at each vertex:

$$\begin{aligned} \mathcal{H}_{\rm int} = \frac{1}{2A} \sum_{\vec{k},\vec{p},\vec{q}} \sum_{s,s'} & c^{\dagger}_{\vec{k}+\vec{q},s} c^{\dagger}_{\vec{p}-\vec{q},s'} c_{\vec{p},s'} c_{\vec{k},s} \\ & \times \left[V^{+}(\vec{q}) + V^{-}(\vec{q}) \sigma^{z}_{ss} \sigma^{z}_{s's'} \right], \end{aligned} \tag{4}$$

where $V^{\pm}(\vec{q}) = (V_{\rm S} \pm V_{\rm D})/2$ and $V_{\rm S,D}$ are the momentum–space interactions between electrons on the same and different sublattices (or layers), respectively. In the monolayer case, the interactions are pseudospin independent ($V_{\rm S} = V_{\rm D}$), whereas in the bilayer and double-layer cases they are pseudospin-dependent because interlayer interactions are weaker than intralayer interactions.

The dependence of the band energy on the momentum-dependent pseudospin configuration is easy to evaluate. From the form of the pseudospinor for a state

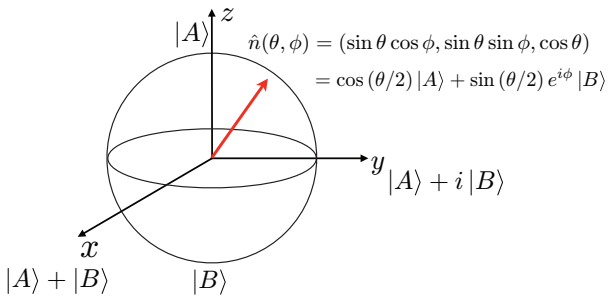

Figure 1. Representation of a pseudospin state by a unit vector $\hat{r}(\theta, \phi)$. Pseudospins directed along the $\pm z$ direction represent the states labeled $|A\rangle$ and $|B\rangle$. For monolayer graphene these states are confined to alternate sublattices, while for bilayer and double-layer graphene they are confined to alternate layers. General pseudospin states are coherent linear combinations of $|A\rangle$ and $|B\rangle$, with the azimuthal pseudospin angle ϕ specifying the phase difference between $|A\rangle$ and $|B\rangle$ amplitudes and the polar pseudospin angle specifying the $|A\rangle - |B\rangle$ polarization. A state with $\theta = \pi/2$ has equal $|A\rangle$ and $|B\rangle$ weights, whereas the states with $\theta = 0$ and $\theta = \pi$ equal $|A\rangle$ and $|B\rangle$, respectively.

aligned in a particular pseudospin direction (see figure 1),

$$|\hat{n}\rangle = \begin{pmatrix} \cos\frac{\theta}{2} \\ \sin\frac{\theta}{2}\, e^{i\phi} \end{pmatrix}, \tag{5}$$

it is easy to show that

$$\langle\hat{n}|\vec{\sigma}\,|\hat{n}\rangle = \hat{n} \tag{6}$$

and that

$$|\hat{n}\rangle\langle\hat{n}| = \frac{1 + \vec{\sigma}\cdot\hat{n}}{2}. \tag{7}$$

In equation (5), θ and ϕ are the polar and azimuthal angles for the pseudospin orientation, i.e. $\hat{n} = (\sin\theta\cos\phi, \sin\theta\sin\phi, \cos\theta)$. In the case of pseudospin-dependent interactions, the following identity is useful:

$$\sigma^z|\hat{n}\rangle\langle\hat{n}|\sigma^z = \frac{1 - \sigma^x n^x - \sigma^y n^y + \sigma^z n^z}{2}. \tag{8}$$

Taking the expectation values of the band and interaction Hamiltonians, we find that

$$E_{\rm band}[\hat{n}_{\vec{k}}] = \sum_{\vec{k}} \vec{h}_{\vec{k}}\cdot\hat{n}_{\vec{k}} \tag{9}$$

and that

$$E_{\rm int}[\hat{n}_{\vec{k}}] = \frac{-1}{4A}\sum_{\vec{k},\vec{p}}\Big[\big(1 + n^z_{\vec{k}} n^z_{\vec{p}}\big)\, V_{\rm S}(\vec{k}-\vec{p}) + \big(n^x_{\vec{k}} n^x_{\vec{p}} + n^y_{\vec{k}} n^y_{\vec{p}}\big)\, V_{\rm D}(\vec{k}-\vec{p})\Big]. \tag{10}$$

The interaction energy is an exchange contribution which sets the momentum transfer $\vec{q}$ in equation (4) to $\vec{p} - \vec{k}$. As explicitly shown in equation (10), the exchange energy contribution from any pair of momentums is lowered when their pseudospins are made more parallel. The band energy, on the other hand, is minimized when the pseudospin direction is opposite to the direction of $\vec{h}_{\vec{k}}$ at every $\vec{k}$ and hence strongly pseudospin dependent (see figure 2). In the following sections we will discuss the pseudospin orientation function which minimizes the total energy $E_{\rm tot} = E_{\rm band} + E_{\rm int}$ for the monolayer, bilayer and double-layer cases.

3. Spin-density-wave states in monolayer graphene

We find it useful to expand the total energy functional to leading order around its band theory value $\hat{n}_{{\rm b}\,\vec{k}} = -\hat{h}_{\vec{k}}$. This consideration follows similar lines in the three cases of interest. To leading order we can preserve normalization by writing

$$\hat{n}_{\vec{k}} = -\hat{h}_{\vec{k}}\left(1 - \tfrac{1}{2}|\vec{\delta}_{\vec{k}}|^2\right) + \vec{\delta}_{\vec{k}}, \tag{11}$$

where $\vec{\delta}_{\vec{k}}$ is a 2D vector perpendicular to $\hat{h}_{\vec{k}}$. For monolayer graphene the band pseudospin orientation $\hat{n}_{{\rm b}\,\vec{k}} = -\hat{k} = -\big(\cos\phi_{\vec{k}}, \sin\phi_{\vec{k}}, 0\big)$ and δ has $\hat{z}$ and azimuthal $(\hat{\phi})$ components along the $\hat{z} = (0,0,1)$ and $\hat{\phi}_{\vec{k}} = \hat{z}\times\hat{k} = \big(\sin\phi_{\vec{k}}, -\cos\phi_{\vec{k}}, 0\big)$ directions, respectively. We find that

$$E = E_0 + \frac{1}{4A}\sum_{\vec{k},\vec{p}}\sum_{\alpha,\beta}\delta^\alpha_{\vec{k}}\, K^{\alpha,\beta}_{\vec{k},\vec{p}}\,\delta^\beta_{\vec{p}}, \tag{12}$$

where

$$K^{\alpha,\beta}_{\vec{k},\vec{p}} = \delta_{\alpha,\beta}\big[2A(h_{\vec{k}} + \Sigma_{\vec{k}})\delta_{\vec{k},\vec{p}} - V_{\rm D}(\vec{k}-\vec{p})\,\hat{\phi}_{\vec{k}}\cdot\hat{\phi}_{\vec{p}}\,\delta_{\alpha,\phi} - V_{\rm S}(\vec{k}-\vec{p})\,\delta_{\alpha,z}\big], \tag{13}$$

where

$$\Sigma_{\vec{k}} = -\frac{\partial E_{\rm tot}[\hat{n}_{\vec{k}}]}{\partial\hat{n}_{\vec{k}}}\cdot\hat{h}_{\vec{k}}. \tag{14}$$

The quantity $\Sigma_{\vec{k}}$ in the above equations, the change in interaction energy associated with switching a single band state from valence to conduction band pseudospin orientations can be identified as the exchange contribution to the self-energy of the band state. $\Sigma_{\vec{k}}$ adds to the energy difference between conduction and valence band states because of the energy cost of reversing pseudospin orientation at a single momentum, keeping all other pseudospins fixed. For the monolayer graphene case, we can let $V_{\rm D} \to V_{\rm S} \to V$ so that

$$\Sigma_{\vec{k}} = \frac{1}{2A}\sum_{\vec{p}} V(\vec{p}-\vec{k})\,\hat{n}_{{\rm b}\,\vec{p}}\cdot\hat{n}_{{\rm b}\,\vec{k}}, \tag{15}$$

which vanishes for a δ-function interaction model because of the angular average over the direction of $\vec{p}$, but grows with $|\vec{k}|$ for the realistic Coulomb interaction case:

$$\Sigma_{\vec{k}} \simeq \frac{\alpha}{4}\,\hbar v_0 k\,\ln(\Lambda/k), \tag{16}$$

where $\alpha = e^2/\epsilon\hbar v_0$ is graphene's fine structure constant, $\Lambda \sim 1/a$ is the Dirac model ultraviolet cutoff where a is graphene's lattice constant, and ϵ is the graphene sheet's effective dielectric constant which depends on the substrate used to support the sheet. Full BZ Hartree–Fock theory calculations [18] suggest that the most appropriate value for Λ is $\sim 30/a$. The self-energy term captures the physics of a theoretically anticipated [18–22] logarithmic interaction

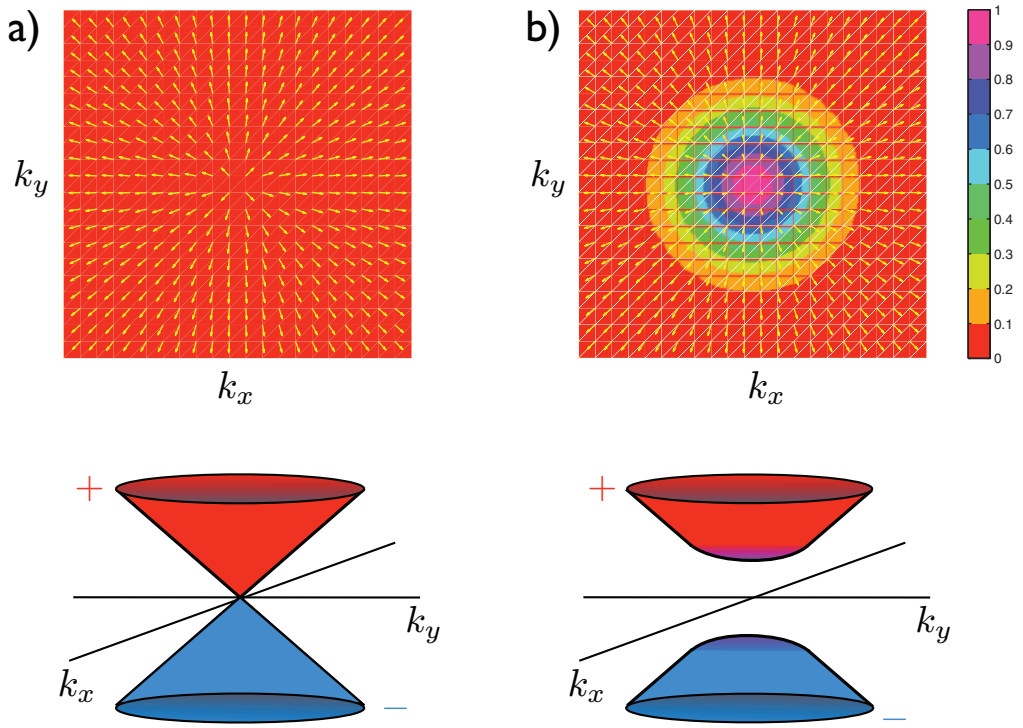

Figure 2. Pseudospin orientations and quasiparticle spectra near the Dirac point for gapless and gapped monolayer graphene. The upper row illustrates conduction band pseudospin orientations for the gapless (a) and gapped (b) cases; the valence band pseudospins are opposite in direction at each momentum. The arrows indicate the magnitude and direction of the $\hat{x}$–$\hat{y}$ plane pseudospin projection, while the color indicates the $\hat{z}$ direction pseudospin projection, which is zero in the gapless unbroken symmetry state. In monolayer graphene pseudospins rotate around the $\hat{z}$-axis by 2π when a point in momentum space encloses the Dirac point $\vec{k} = 0$. In the broken symmetry state the self-energy contribution to the pseudospin field has a component in the $\hat{z}$ direction, which does not vanishes for $k \to 0$, opening up a gap in the quasiparticle spectrum.

enhancement of the energy difference between conduction and valence band quasiparticles, which has now been confirmed experimentally [23]. This effect that is normally described in terms of an interaction-enhanced quasiparticle velocity at momenta near the Dirac points.

Depending on the dielectric environment of a monolayer graphene sheet, the fine structure constant value can vary between $\alpha \sim 0.5$ and $\alpha \sim 2$ [24]. It is sometimes claimed that perturbative and mean-field treatment of electron–electron interaction effects, like the one discussed here, cannot be trusted because the coupling constant is not small. A more reliable way of judging the adequacy of these approximations is to compare with experiments. In the case of monolayer graphene, the application of this type of criteria usually argues for the opposite conclusion, namely that mean-field theory is reliable, provided that the electron–electron interaction is properly screened when carriers are present. The approximation in which electronic self-energies are approximated at leading order in dynamically screened Coulomb interactions, variously known as the random phase approximation (RPA) or the *GW* approximation, agrees very well with, in particular, photoemission experiments [25] in both neutral and charged monolayer graphene. For neutral graphene the inverse quasiparticle lifetime [26, 27] in neutral graphene is ∼10% of the quasiparticle energy at typical values of α, and this ratio may provide a better characterization of interaction strength.

Although some details of graphene interaction physics are sensitive to the long range of Coulomb interactions [18, 28–30], most importantly perhaps the velocity enhancement mentioned above, we are able to make a number of valuable points by considering a short-range interaction model in which the momentum dependences of V_S and V_D are neglected. Note that because we are neglecting inter-valley scattering we are still imagining that the interaction range is large compared to the atomic length scale, and that there is therefore no direct relationship between this approximation and using a lattice Hubbard model [43–46]. Setting $V_S = V_D \to U$, we find that Σ vanishes, that

$$K^{\phi,\phi}_{\vec{k},\vec{p}} \to 2A\hbar v_0 k \delta_{\vec{k},\vec{p}} - U\hat{\phi}_{\vec{k}} \cdot \hat{\phi}_{\vec{p}} \tag{17}$$

and that

$$K^{zz}_{\vec{k},\vec{p}} \to 2A\hbar v_0 k \delta_{\vec{k},\vec{p}} - U. \tag{18}$$

In-plane and out-of-plane pseudospin reorientation instabilities are indicated by vanishing eigenvalues for $K^{\phi,\phi}_{\vec{k},\vec{p}}$ and $K^{zz}_{\vec{k},\vec{p}}$, respectively. We search for a zero eigenvalue by solving

$$\frac{1}{A}\sum_{\vec{p}} K^{\alpha,\alpha}_{\vec{k},\vec{p}} \delta^{\alpha}_{\vec{p}} \equiv 0. \tag{19}$$

These homogeneous equations are solved by setting $\delta^{\phi}_{\vec{p}} \to C\cos(\phi_{\vec{p}} - \chi)/\hbar v_0 k$ and $\delta^{z}_{\vec{p}} \to C/\hbar v_0 k$, where C is an arbitrary constant and χ an arbitrary angle. We obtain the conditions

$$2\cos(\phi_{\vec{k}} - \chi) = U \int \frac{\mathrm{d}\vec{p}}{(2\pi)^2} \frac{\cos(\phi_{\vec{p}} - \phi_{\vec{k}})\cos(\phi_{\vec{p}} - \chi)}{\hbar v_0 p} \tag{20}$$

for $K^{\phi,\phi}$ and

$$2 = U \int \frac{\mathrm{d}\vec{p}}{(2\pi)^2} \frac{1}{\hbar v_0 p} \tag{21}$$

for $K^{z,z}$. Converting the integral over momentum $\vec{p}$ into an integral over the energy of quasiparticles with energy $\hbar v_0 p$, it follows that instability occurs in $K^{\phi,\phi}$ when $U\nu^* > 4$, whereas for $K^{z,z}$ it occurs when $U\nu^* > 2$. In these equations, $\nu^* = W/(2\pi\hbar^2 v_0^2)$ is the Dirac-model density-of-states at the model's ultraviolet energy cutoff scale $W \sim \hbar v_0/a$; the integrand of the energy integral is constant because of a cancellation between the $\hbar v_0 p$ factor in the denominator and the quasiparticle density-of-states, which is proportional to energy. Interactions are less effective in reducing the energy cost of in-plane ϕ distortions than out-of-plane z distortions because of the angle dependence of the band state pseudospins.

There are two important points to make about these stability criteria results. First of all, we see that if interactions are strong, pseudospins are more likely to tilt toward the $\pm\hat{z}$ directions, rather than to alter their orientations in the $\hat{x}$–$\hat{y}$ plane. The state produced by this pseudospin distortion has a higher electron density on one sublattice than the other; hence, it is a density-wave state when looked at from a microscopic point of view. In ignoring the Hartree energy, we have implicitly assumed that the signs of the density waves are opposite for opposite valleys or for opposite spins, with the latter possibility being more likely as we discuss later. The expected state is therefore a spin-density-wave state rather than a charge-density-wave state. If the instability involved distortion of the in-plane pseudospin direction, rather than tilting out of the plane, it would yield a state with spontaneous anisotropy, characterized by the angle χ, in which the magnitude of the quasiparticle self-energy depends on the momentum direction. The mean-field-theory instability analysis therefore suggests that density-wave instabilities occur before anisotropy instabilities. Secondly, we note that the instability criterion involves ν^*, the density-of-states at the band width energy scale. We can conclude from this observation that the presence or absence of a broken symmetry state depends on atomic length scale physics beyond that captured by the $\vec{k}\cdot\vec{p}$ Dirac model [13, 17, 18].

When solved with an unscreened Coulomb interaction [5], mean-field theory predicts that the instability occurs in monolayer graphene at $\alpha \sim 1.3$; screening and other higher-order corrections will shift (for a discussion of estimates, see [31] and references therein) the instability—likely to larger values of α beyond those that can be reached in monolayer graphene even when it is suspended so that interactions are not reduced by dielectric screening. Degrees of freedom not included in the π-band only model of graphene and portions of the BZ far from the the corner Dirac points are also likely to play an important role. The instability can also be ruled out experimentally with nearly complete confidence because pseudospin orientations in the $\hat{z}$ direction open gaps in the quasiparticle spectrum. It can be established experimentally that the gaps, if present, cannot be larger than $\sim 10^{-4}$ eV compared to the natural energy scale of graphene, which is $\sim$10 eV [32].

4. Antiferromagnetic states in bilayer graphene

Several consequential distinctions can be drawn between the monolayer and bilayer cases. First of all, the two-band $\vec{k}\cdot\vec{p}$ for the bilayer model provides a good description only at energies that are small compared to the interlayer tunneling energy $\gamma_1 \sim 0.4$ eV, whereas the corresponding monolayer two-band model applies up to energies $\sim$2 eV, much closer to the full band width. Secondly, both the magnitude and direction of pseudospin effective magnetic fields have different behaviors since $\vec{h}^{(\mathrm{BL})}_{\vec{k}}$ varies quadratically rather than linearly with k and has an orientation angle that is twice the momentum orientation angle. The stability analysis for bilayers parallels the strategy used in the single-layer case once these differences are recognized. For bilayers the band and in-plane-distortion pseudospin directions are $\hat{n}_{\mathrm{b}\vec{k}} = \big(\cos(2\phi_{\vec{k}}), \sin(2\phi_{\vec{k}}), 0\big)$ and $\hat{\phi}_{\vec{k}} = \hat{n}_{\mathrm{b}\vec{k}} \times \hat{z} = \big(\sin(2\phi_{\vec{k}}), -\cos(2\phi_{\vec{k}}), 0\big)$. The more rapid variation of the pseudospin direction with the momentum direction eliminates the logarithmic divergence of the velocity enhancement at small k found in the monolayer Coulomb interaction case, but still [22] leaves a substantial interaction-induced velocity enhancement. For the short-range interaction model, the stability matrices for ϕ and z distortions are

$$K^{\phi,\phi}_{\vec{k},\vec{p}} \to 2A \frac{\hbar^2 k^2}{2m^*} \delta_{\vec{k},\vec{p}} - U \hat{\phi}_{\vec{k}} \cdot \hat{\phi}_{\vec{p}} \tag{22}$$

and

$$K^{zz}_{\vec{k},\vec{p}} \to 2A \frac{\hbar^2 k^2}{2m^*} \delta_{\vec{k},\vec{p}} - U, \tag{23}$$

where $\hat{\phi}_{\vec{k}} \cdot \hat{\phi}_{\vec{p}}$ now equals $\cos(2\phi_{\vec{p}} - 2\phi_{\vec{k}})$. Setting $\delta^{\phi}_{\vec{p}} \to C\cos(2\phi_{\vec{p}} - \chi)/(\hbar^2 p^2/2m^*)$ and $\delta^{z}_{\vec{p}} \to C/(\hbar^2 p^2/2m^*)$, we can solve for the interaction strength at which the smallest eigenvalue approaches zero. As in the monolayer case, we find that the $\pm\hat{z}$ distortions, which in this case correspond to moving charge between layers, occur at weaker interaction strengths. The instability criteria [6] in the bilayer case are $U\nu^{\mathrm{BL}}\ln(W/E_{\mathrm{F}}) > 4$ for $K^{\phi,\phi}$ and $U\nu^{\mathrm{BL}}\ln(W/E_{\mathrm{F}}) > 2$ for $K^{z,z}$. In this case $\nu^{\mathrm{BL}} = m^*/(2\pi\hbar^2)$ is the energy-independent band electron density-of-states. The $1/E$ quasiparticle energy factor is not canceled by an increasing density-of-states, as it was in the monolayer case, and the interaction contribution to the stability eigenvalue integral has a logarithmic infrared divergence which we have cut off by assuming that conduction band states up to energy E_{F} have been occupied, Pauli-blocking pseudospin polarization. For $E_{\mathrm{F}} \to 0$ the conclusion is that the density-wave instability occurs before the anisotropy distortion, as illustrated in figure 3, and that it will occur for arbitrarily weak interactions [5–7].

5. Exciton condensates in double-layer graphene

Now we turn to the case in which two graphene layers, one containing electrons in the conduction band and the other containing an equal density of holes in the valence band, are coupled by repulsive Coulomb interactions. If we ignore the completely full and completely empty energetically remote bands, we can view the double-layer graphene system using the same pseudospin language that we used for the monolayer

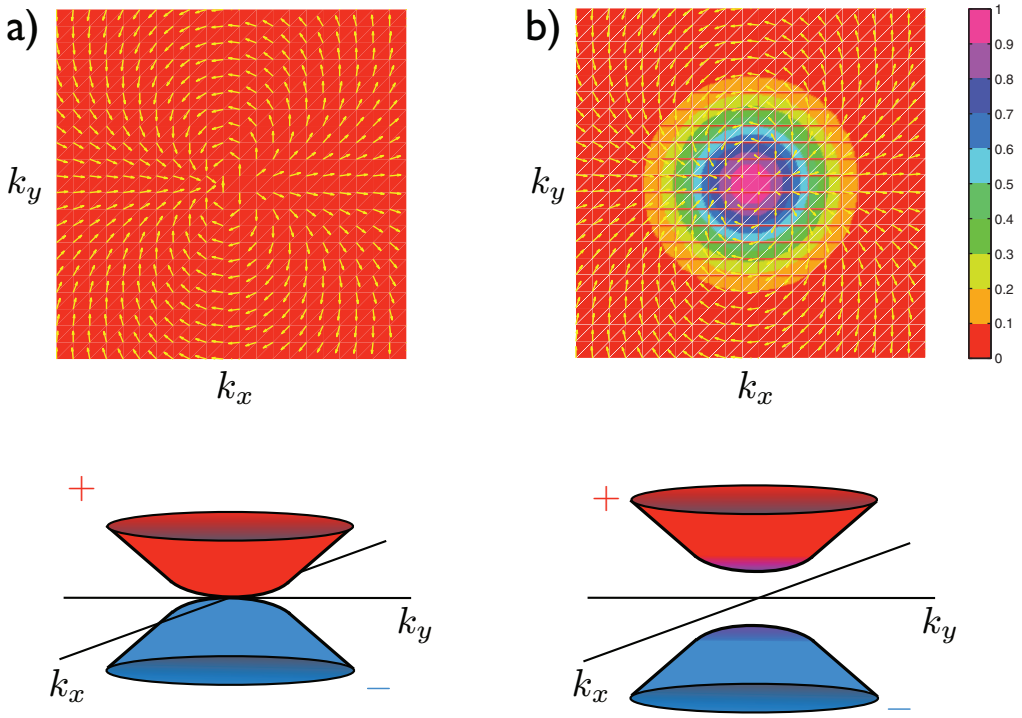

Figure 3. Pseudospin orientations and quasiparticle dispersions near the Dirac point in bilayer graphene. The upper row illustrates the conduction band pseudospin orientations; the valence band pseudospin orientation is opposite at each momentum. In bilayer graphene pseudospins rotate by an angle of 4π around the $\hat{z}$ direction when a point in momentum space encloses the $\vec{k} = 0$ Dirac point. Panels (a) and (b) represent gapless and gapped broken symmetry states, respectively. As in the monolayer case all pseudospins are in the x–y plane in the ungapped state. In the gapful case the $\pm\hat{z}$ out of plane pseudospin components are nonzero and indicate sublattice polarization. Because the low-energy $\vec{k}\cdot\vec{p}$ model of bilayer graphene includes only two sites per unit cell, the sublattice pseudospin label equivalent to a layer label.

and bilayer graphene cases. In the absence of interactions the conduction band states of the n-layer, which we associate with pseudospin up, are occupied inside a Fermi circle and the valence band states of the p-layer, which we associate with pseudospin down, are occupied outside of this circle (see figure 4). As in the monolayer and bilayer cases, one pseudospin state is occupied at each momentum. Because the band pseudospins are oriented in the $\pm\hat{z}$ directions, rather than in the $\hat{x}$–$\hat{y}$ plane, the pseudospin distortions that can potentially lower the energy are in the $\hat{x}$ and $\hat{y}$ direction distortions, rather than $\hat{\phi}$ and $\hat{z}$ distortions. We find that

$$K^{x,x}_{\vec{k},\vec{p}} = K^{y,y}_{\vec{k},\vec{p}} = [2A(\hbar v_0(k-k_F) + \Sigma_{\vec{k}})\delta_{\vec{k},\vec{p}} - V_D(\vec{k}-\vec{p})], \tag{24}$$

where

$$\Sigma_{\vec{k}} = \frac{n^z_{\mathrm{b}\vec{k}}}{2A}\sum_{\vec{p}} V_{\mathrm{S}}(\vec{p}-\vec{k})\,(1+n^z_{\mathrm{b}\vec{p}}). \tag{25}$$

(We take the band energy to be the quasiparticle energy in the absence of carriers in either layer and include a self-energy contribution from the full valence band of the n-type layer.) The sudden change in pseudospin orientation at the Fermi circle has a cost in exchange energy which can be mitigated by rotating pseudospins into the $\hat{x}$–$\hat{y}$ plane, which corresponds to establishing coherence between layers spontaneously. Because $K^{x,x} = K^{y,y}$, the pseudospin rotation can occur with the same gain in energy at any azimuthal angle. The fact that the energy is independent of the interlayer phase (i.e. the pseudospin azimuthal angle) implies that this broken symmetry state supports supercurrents that flow in opposite directions in opposite layers [4, 16]. As in the monolayer and bilayer cases, instability is indicated by a vanishing $K^{x,x}_{\vec{k},\vec{p}}$ eigenvalue. The instability condition can be found by solving

$$\frac{1}{A}\sum_{\vec{p}} K^{x,x}_{\vec{k},\vec{p}}\delta^x_{\vec{p}} \equiv 0 \tag{26}$$

with $\delta^x_{\vec{p}} \to C/\hbar v_0|k-k_F|$. For a δ-function interaction the self-energy term simply shifts the relationship between Fermi energy and density and plays no role. The instability criterion is therefore $U\nu^{\mathrm{DL}}\ln(2E_{\mathrm{F}}/\delta) > 2$ where we have chosen $2E_{\mathrm{F}}$ as an ultraviolet cutoff, δ is an infrared cutoff, and $\nu^{\mathrm{DL}} = E_{\mathrm{F}}/(2\pi\hbar^2 v_0^2)$ is the constant density-of-states of the double-layer Dirac model for energies between 0 and E_{F}. As in the bilayer case, an instability occurs for arbitrarily weak interactions. Although this conclusion is universally accepted by researchers who have examined this possible ordered state [4, 33–36], estimates of the size of the consequent energy gap vary widely because of the difficulty of accounting accurately for the influence of carrier screening.

6. Discussion

Graphene 2DES are remarkable for several different reasons. The fact that they are truly 2D on an atomic length scale elevates 2DES physics from the low-temperature world to the room-temperature world. Furthermore, they

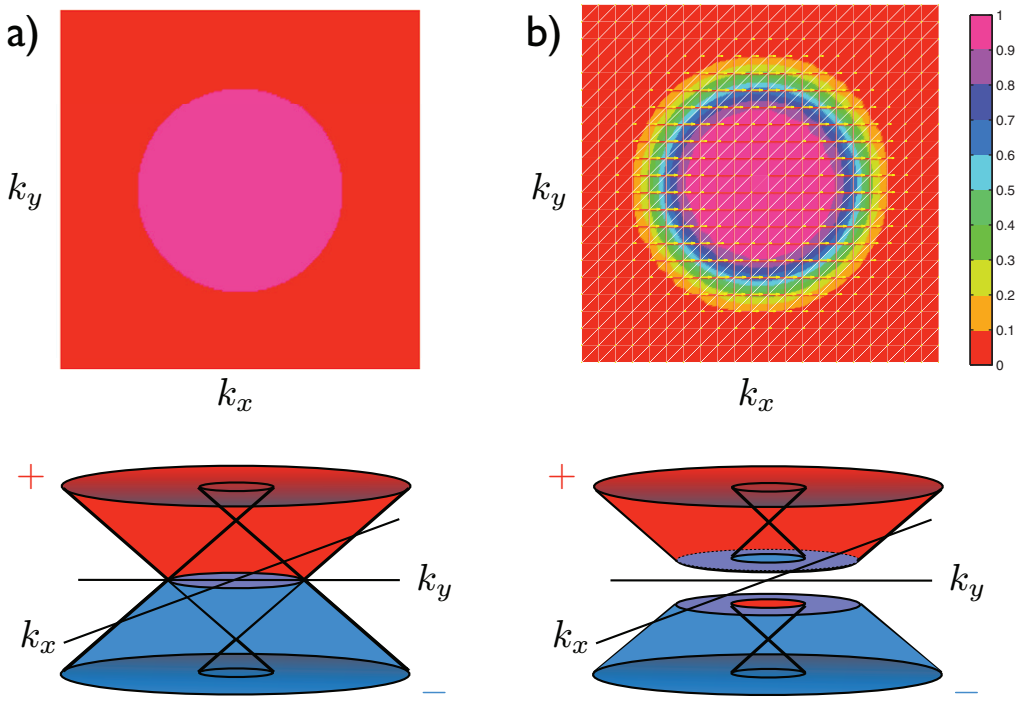

Figure 4. Pseudospin orientations and quasiparticle dispersions in double-layer graphene near the Dirac point. In the two-band pseudospin model, the two bands furthest from the Fermi energy are not accounted for explicitly. In double-layer graphene tunneling between layers is negligible so that the pseudospin label is equivalent to a layer label. The band pseudospin direction changes abruptly between up and down directions along the common Fermi surface where the conduction band of the high-density layer and the valence band of the low-density layer cross. In the presence of interactions a gap is opened and pseudospin directions rotate gradually between up and down directions. Panels (a) and (b) represent, respectively, the single particle bands crossing at a Fermi circle and the gapped phase with interlayer coherence. A gap opens in the presence of arbitrarily weak interactions as in the case of bilayer graphene. Any in-plane pseudospin component introduces interlayer coherence and reduces the total energy of the system. In our illustration, we have chosen the interlayer coherence pseudospin component to point in the x direction.

are accurately described by very simple models over very wide energy ranges and yet have electronic properties that can be qualitatively altered simply by stacking [3, 37–40] them in different arrangements, and by adjusting external gate voltages. In this paper we have discussed the properties of three different graphene 2DES using a simple mean-field-theory pseudospin language and specializing to the case of electrically neutral systems.

The basic building block of all graphene 2DES is the isolated monolayer, which is described by a massless Dirac $\vec{k}\cdot\vec{p}$ Hamiltonian over a wide energy range. The Dirac model has chiral quasiparticles, and in the graphene case the chirality refers to the relationship between $\vec{k}\cdot\vec{p}$ momentum and the direction of a pseudospin associated with the sublattice degree-of-freedom of graphene's honeycomb lattice [5, 41]. In neutral graphene each momentum is singly occupied on average. In our mean-field-theory approach we do not account for quantum fluctuations in these momentum occupation numbers, but allow energy to be minimized with respect to the pseudospin orientation at each momentum. Using this approach we find that in monolayer graphene strong interactions can lead to a broken symmetry state in which the pseudospin rotates from the $\hat{x}$–$\hat{y}$ plane toward the $\pm\hat{z}$ directions, breaking inversion symmetry and opening up a gap in the quasiparticle excitation spectrum. This conclusion has previously been reached (see, for example [42] and references therein) [18, 43–46] by several researchers, sometimes using more sophisticated theoretical approaches which attempt quantitative estimates of the required interaction strengths. In $\vec{k}\cdot\vec{p}$ mean-field theory the broken symmetry state consists of a density-wave state with more charge on one sublattice than the other within each spin-valley flavor, but no overall charge density variation. Since exchange interactions beyond the $\vec{k}\cdot\vec{p}$ level favor [13] states with the same sublattice polarization on both valleys, the strong interaction state is likely a spin-density-wave state. As it happens, it appears to be clear from experiment that this broken symmetry state does not occur [23, 25] in monolayer graphene, even when suspended. This property is generally consistent with theoretical expectations and is perhaps unfortunate from the point of view of researchers interested in many-body phenomena. Happily the very closely related bilayer and double-layer graphene systems that were not anticipated prior to the experimental emergence of the graphene field are more likely to have broken symmetry states and may save the day for interesting many-body phenomena in graphene-based 2DES.

Bilayer graphene is described, over a more limited energy range however, by a similar pseudospin $\vec{k}\cdot\vec{p}$ model with quadratic rather than linear dispersion; in bilayer graphene the quasiparticle velocity vanishes with momentum as in a conventional 2DES, but the pseudospin direction still depends on the direction of momentum. In pseudospin language, it is clear that the bilayer is more susceptible to instabilities to broken symmetry states because the cost in band energy of rotating the pseudospins toward the $\pm\hat{z}$ direction is smaller

at small momentum. Indeed we find that instabilities occur for arbitrarily weak interactions [5, 6]. In the bilayer case the spin-density-wave state has opposite pseudospin orientations for opposite spins [12–14]. An alternate state in which the pseudospin orientation is rotated within the $\hat{x}$–$\hat{y}$ plane to increase the degree of alignment leads to an anisotropic state, and gains less exchange energy for a given interaction energy cost. There is indeed a great deal of evidence from recent experiments [48, 49] that a broken symmetry state does occur in bilayer graphene, but the character of the state is not yet completely settled since some experimenters find evidence for a gapless anisotropic state [47] and others [50, 51] evidence for a gapped isotropic state [5–7, 13]. On the theoretical side, different researchers have also reached different conclusions concerning the character of these states, with some researchers [8, 9] concluding that the broken symmetry state should be anisotropic.

In mean-field theory, the gapped broken symmetry state has lower energy than the anisotropic broken symmetry state because all band pseudospinors can be tilted to the $\pm\hat{z}$ direction to reduce the probability of finding electrons with parallel pseudospins. The efficacy of in-plane pseudospin distortions is reduced because their pseudospin directions $\hat{\phi}_{\vec{k}}$ depend on the momentum orientation angle $\phi_{\vec{k}}$. To us, the conclusion that the weak-coupling broken symmetry state will be gapped appears to be unavoidable unless somehow overturned, in a way which has not yet been clearly articulated, by inter-flavor correlations. In drawing conclusions from the renormalization group calculations [6, 8, 9] which attempt to go beyond the mean-field theory considerations described here, it is important to realize that, because short-range interactions within a valley act only between opposite pseudospins, the pseudospin dependence of the corresponding flowing interaction has no significance in a many-fermion Hilbert space.

Bilayer graphene differs from monolayer graphene mainly because of its weaker dependence of band energy on pseudospin direction at small momentum. This difference is sufficient to lead to states with broken pseudospin symmetry. Double-layer graphene differs in a more qualitative way because not only the interaction energy, but also the band energy, is diagonal in the $\hat{z}$ component of pseudospin, i.e. in the layer index. The band Hamiltonian in this case has a sudden change in the sign of the $\hat{z}$ direction pseudospin orientation. This momentum space *domain wall* has a large interaction energy cost, which can be mitigated by rotating the pseudospins near the Fermi surface out of the $\hat{z}$ direction with a common azimuthal angle. In this way, the momentum dependence of the pseudospin rotates smoothly between the $\hat{z}$ and $-\hat{z}$ directions, and the interaction energy is lowered. Like bilayer graphene, double-layer graphene has a broken symmetry for arbitrarily weak interactions. In both cases the size of the gap is difficult to estimate quantitatively [4, 33–36] and likely to be overestimated by mean-field theory. The quasiparticle density of states at the Fermi level in double-layer graphene is finite because the bands cross along a line in momentum space. In bilayer graphene the bands cross at a point, but the density of states is still finite because the band dispersion is quadratic. The consequences for order in the two cases are however essentially the same.

In 2DES, the quantized Hall conductance can be expressed [52] in terms of an integral of Berry curvature over momentum space. Using ideas from topology it is possible to show that the Hall conductivity is always e^2/h times an integer valued topological invariant known as the Chern number. For two-band models, momentum states can always be described using a pseudospin-1/2 language like the one used in this paper. For this case the quantized Hall conductivity is especially simple to visualize geometrically since it is equal to the number of times the unit sphere of pseudospin directions is covered upon integrating over momentum space. The broken symmetry states of bilayer graphene carry a positive or negative unit of Hall conductivity because they cover either the north pole or the south pole twice when the pseudospin at $\vec{k} = 0$ points to the north or south pole. (In the double-layer graphene case, on the other hand, the pseudospin is confined to the interface between a plane and the pseudospin unit sphere, i.e. to a line on the unit sphere that encompasses zero area.) The inversion symmetry breaking states in bilayer graphene can therefore be viewed as spontaneous quantum Hall states [11–13]. In the spin-density-wave state the Hall contributions from different valleys cancel, but states with a nonzero Hall conductivity can be stabilized by going to a nonzero total carrier density in weak magnetic fields.

In this paper, we have discussed the possibility of interaction-driven broken symmetries in three different graphene-based 2DES, monolayer graphene systems and two-layer graphene systems that are stacked in two different ways. The three cases we have discussed are most easily addressed theoretically, but not by any means the ones that are most likely to have strong interaction effects and broken symmetries. ABC stacked multilayers [37–39], for example, tend to have even smaller separations between conduction and valence bands at small $|\vec{k}|$, but are complicated by competing electronic structure details. Recent advances in techniques for preparing samples in which disorder plays an inessential role appear to be bringing us close to clear experimental conclusions as to the strength and character of broken symmetries in bilayers and trilayers. These developments will, no doubt, reveal some surprises that present some focused challenges to theory.

References

[1] Geim A K and MacDonald A H 2007 *Phys. Today* **60** 35
[2] Castro Neto A H, Guinea F, Peres N M R, Novoselov K S and Geim A K 2009 *Rev. Mod. Phys.* **81** 109
[3] McCann E and Fal'ko V I 2006 *Phys. Rev. Lett.* **96** 086805
[4] Min H, Bistritzer R, Su J and MacDonald A H 2008 *Phys. Rev.* B **78** 121401
[5] Min H, Borghi G, Polini M and MacDonald A H 2008 *Phys. Rev.* B **77** 041407
[6] Zhang F, Min H, Polini M and MacDonald A H 2010 *Phys. Rev.* B **81** 041402
[7] Nandkishore R and Levitov L 2010 *Phys. Rev. Lett.* **104** 156803
[8] Vafek O and Yang K 2010 *Phys. Rev.* B **81** 041401
[9] Lemonik Y, Aleiner I L, Toke C and Fal'ko V I 2010 *Phys. Rev.* B **82** 201408
[10] Xiao D, Yao W and Niu Q 2007 *Phys. Rev. Lett.* **99** 236809
Xiao D, Chang M-C and Niu Q 2010 *Rev. Mod. Phys.* **82** 1959
[11] Nandkishore R and Levitov L 2010 *Phys. Rev.* B **82** 115124

[12] Zhang F, Jung J, Fiete G A, Niu Q and MacDonald A H 2011 *Phys. Rev. Lett.* **106** 156801
[13] Jung J, Zhang F and MacDonald A H 2011 *Phys. Rev.* B **83** 115408
[14] Zhang F and MacDonald A H 2011 arXiv:1107.4727
[15] Eisenstein J P and MacDonald A H 2004 *Nature* **432** 691
[16] Su J-J and MacDonald A H 2008 *Nature Phys.* **4** 799
[17] Jung J and MacDonald A H 2009 *Phys. Rev.* B **80** 235417
[18] Jung J and MacDonald A H 2011 *Phys. Rev.* B **84** 085446
[19] Abrikosov A A and Beneslavskii S D 1970 *Zh. Eksp. Teor. Fiz.* **59** 1280
Abrikosov A A and Beneslavskii S D 1971 *Sov. Phys.—JETP* **32** 699
[20] Gonzalez J, Guinea F and Vozmediano M A H 1999 *Phys. Rev.* B **59** R2474
Gonzalez J, Guinea F and Vozmediano M A H 1996 *Phys. Rev. Lett.* **77** 3589
Gonzalez J, Guinea F and Vozmediano M A H 1994 *Nucl. Phys.* B **424** 595
Gonzalez J, Guinea F and Vozmediano M A H 1994 *J. Low Temp. Phys.* **99** 287
Vozmediano M A H, Lopez-Sancho M P, Stauber T and Guinea F 2005 *Phys. Rev.* B **72** 155121
Guinea F, Castro A H and Neto Peres N M R 2007 *Eur. Phys. J. Spec. Top.* **148** 117
[21] Barlas Y, Pereg-Barnea T, Polini M, Asgari R and MacDonald A H 2007 *Phys. Rev. Lett.* **98** 236601
[22] Borghi G, Polini M, Asgari R and MacDonald A H 2009 *Solid State Commun.* **149** 1117
[23] Elias D C, Gorbachev R V, Mayorov A S, Morozov S V, Zhukov A A, Blake P, Novoselov K S, Geim A K and Guinea F 2011 *Nature Phys.* **7** 701
[24] Jang C, Adam S, Chen J-H, Williams E D, Das Sarma S and Fuhrer M S 2008 *Phys. Rev. Lett.* **101** 146805
[25] Bostwick A, Speck F, Seyller T, Horn K, Polini M, Asgari R, MacDonald A H and Rotenberg E 2010 *Science* **328** 999
[26] Trevisanutto P E *et al* 2008 *Phys. Rev. Lett.* **101** 226405
[27] Polini M, Asgari R, Borghi G, Barlas Y, Pereg-Barnea T and MacDonald A H 2008 *Phys. Rev.* B **77** 081411
[28] Honerkamp C 2008 *Phys. Rev. Lett.* **100** 146404
[29] Herbut I F 2006 *Phys. Rev. Lett.* **97** 146401
Herbut I F, Juricic V and Roy B 2009 *Phys. Rev.* B **79** 085116
Juricic V, Herbut I F and Semenoff G W 2009 *Phys. Rev.* B **80** 081405
[30] Wehling T O, Şaşıoğlu E, Friedrich C, Lichtenstein A I, Katsnelson M I and Blügel S 2011 *Phys. Rev. Lett.* **106** 236805
[31] Gonzalez J 2011 arXiv:1103.3650
[32] Bolotin K I, Ghahari F, Shulman M D, Stormer H L and Kim P 2009 *Nature* **462** 196
[33] Zhang C-H and Joglekar Y N 2008 *Phys. Rev.* B **77** 233405
[34] Lozovik Yu E and Sokolik A A 2007 *JETP Lett.* **87** 55
Lozovik Yu E and Sokolik A A 2008 *J. Phys.: Conf. Ser.* **129** 012003
Berman O L, Lozovik Y E and Gumbs G 2008 *Phys. Rev.* B **77** 155433
[35] Kharitonov M Yu and Efetov K B 2008 *Phys. Rev.* B **78** 241401
Kharitonov M Yu and Efetov K B 2010 *Semicond. Sci. Technol.* **25** 034004
[36] Dillenschneider R and Han J H 2008 *Phys. Rev.* B **78** 045401
[37] Min H and MacDonald A H 2008 *Phys. Rev.* B **77** 155416
[38] Min H and MacDonald A H 2008 *Prog. Theor. Phys. Suppl.* **176** 227
[39] Zhang F, Sahu B, Min H and MacDonald A H 2010 *Phys. Rev.* B **82** 035409
[40] Guinea F, Castro Neto A H and Peres N M R 2006 *Phys. Rev.* B **73** 245426
[41] Trushin M and Schliemann J 2011 *Phys. Rev. Lett.* **107** 156801
[42] Herbut I F 2006 *Phys. Rev. Lett.* **97** 146401
Drut J E and Lahde T A 2009 *Phys. Rev.* B **79** 165425
Semenoff G W 2012 *Phys. Scr.* **T146** 014016
[43] Fujita M, Wakabayashi K, Nakada K and Kusakabe K 1996 *J. Phys. Soc. Japan* **65** 1920
[44] Sorella S and Tosatti E 1992 *Europhys. Lett.* **19** 699
Martelo L M, Dzierzawa M, Siffert L and Baeriswyl D 1997 *Z. Phys.* B **103** 335
[45] Paiva T, Scalettar R T, Zheng W, Singh R R P and Oitmaa J 2005 *Phys. Rev.* B **72** 085123
[46] Meng Z Y, Lang T C, Wessel S, Assaad F F and Muramatsu A 2010 *Nature* **464** 847
[47] Mayorov A S, Elias D C, Mucha-Kruczynski M, Gorbachev R V, Tudorovskiy T, Zhukov A, Morozov S V, Katsnelson M I, Geim A K and Novoselov K S 2011 *Science* **333** 860
[48] Martin J, Feldman B E, Weitz R T, Allen M T and Yacoby A 2010 *Phys. Rev. Lett.* **105** 256806
[49] Weitz R T, Allen M T, Feldman B E, Martin J and Yacoby A 2010 *Science* **330** 812
[50] Velasco J Jr *et al* 2011 arXiv:1108.1609
[51] Freitag F, Trbovic J, Weiss M and Schönenberger C 2011 arXiv:1104.3816
[52] Thouless D J, Kohmoto M, Nightingale M P and Den Nijs M 1982 *Phys. Rev. Lett.* **49** 405